A STUDY OF COMBUSTION

IN

SUPERSONIC STREAMS

by

FREDERICK STUCKY BILLIG

Thesis submitted to the Faculty of the Graduate School
of the University of Maryland in partial fulfillment
of the requirements for the degree of
Doctor of Philosophy
1964

APPROVAL SHEET

Title of Thesis: A Study of Combustion in Supersonic Streams

Name of Candidate: Frederick Stucky Billig
Doctor of Philosophy, 1964

Thesis and Abstract Approved: 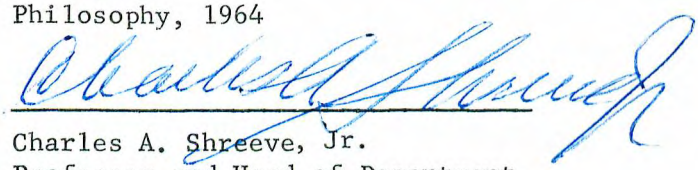

Charles A. Shreeve, Jr.
Professor and Head of Department
Mechanical Engineering

Date Approved: 4 Dec/64

ABSTRACT

Title of Thesis: A Study of Combustion in Supersonic Streams

Frederick Stucky Billig, Doctor of Philosophy, 1964

Thesis directed by: Professor and Head of Department of Mechanical Engineering, Charles A. Shreeve, Jr.

Supervised

Supersonic combustion of reactive aluminum alkyl fuels has been experimentally demonstrated in two-dimensional ducted combustors and adjacent to a flat plate. Fuel was injected from the combustor walls through multiple orifices and ignited spontaneously. Stable supersonic heat release was maintained as evidenced by schlieren and direct motion pictures of the flow field and deduced from static and pitot pressure measurements in the combustion zone.

The results of the ducted combustor tests were correlated with elementary one-dimensional and pseudo-one-dimensional theoretical models of the flow field. This agreement permitted a reasonable determination of combustion efficiency to be made. In the ducted combustor tests a favorable effect of preheating the fuel to approximately 250^{o}F was noted and a simple empirical factor was found which satisfactorily correlated all of the data for the range of conditions tested.

A theoretical model of constant pressure heat release on a flat plate in supersonic flow is postulated. Normal force coefficients and specific impulse values are tabulated for a variety of flight Mach numbers and altitudes. Additional refinements in this theoretical model were required to adequately describe the experimental results. In a test simulating Mach 5 flight at 66,000 feet altitude a side force specific impulse of 1350 seconds was measured at equivalence ratio of

one. Combustion was only partially completed 12 inches downstream of fuel injection. Based on the theoretical model an additional 12 inches of combustor length and 36 inches of expansion length would be required to obtain the estimated theoretical impulse of 5760 sec.

The interaction of a vaporizing liquid droplet with a supersonic stream is considered. Additional refinements were made in the existing theories on droplet trajectory to include the influences of a separated zone and the normal component of velocity of the external stream. Calculations of the trajectory and evaporation of the estimated mean droplet size based on the modified technique were in general agreement with the observed flame zone and deduced combustion efficiency.

ACKNOWLEDGMENT

The research that is presented in this thesis is a result of experiments conducted for the past two years at the Applied Physics Laboratory of The Johns Hopkins University where the author has been a full-time employee. The work has been supported by the Bureau of Weapons, Department of the Navy, under Contract NOw-62-0605-c.

The author gratefully acknowledges the guidance and the advice of Professor Charles A. Shreeve, Jr. and Dr. Gordon L. Dugger in planning the experimental work and preparing of the manuscript. Thanks are due to Mr. R. K. Stiles for assistance with the experimental work and Mr. L. L. Perini for programming the theoretical calculations on the 7094 computer. Finally, thanks are due to Mrs. Anne M. Mack for typing the thesis.

TABLE OF CONTENTS

LIST OF TABLES

LIST OF FIGURES

LIST OF SYMBOLS

a	speed of sound, ft/sec
A	area, ft^2
C_N	normal force coefficient
d_j	injector diamter, cm
d_0	volume mean initial droplet diameter, cm
ER	equivalence ratio = $f/f_{stoichiometric}$
f	fuel/air weight ratio
F_N	normal force, lb_F
g	gravitational constant = 32.16 ft/sec^2
h	special enthalpy, BTU/lb
I_{sp}	normal force specific impulse, $lb_F/(lb/sec)$
J	mechanical equivalent of heat 778 ft-lb/BTU
M	Mach number
p	pressure lb/ft^2 (or psia if specified)
Δp	pressure change, lb/ft^2
q	dynamic pressure = $\rho u^2/2$ lb/ft^2
T	temperature, ^oR (or ^oF if specified)
u	velocity, ft/sec
$\dot{w}$	weight flow, lb/sec
Z	altitude, ft
α	angle between airstream and injectant, degrees
δ	deflection angle, degrees
ϵ	correction factor defined in Eq. (v)
θ	shock angle, degrees
μ	Mach angle, degrees or viscosity, poise
ρ	density, $slugs/ft^3$ or grm/cc

τ	shear stress, lb/ft^2

subscripts

a	streamtube entrance
b	streamtube exit
g	gas (air in this case)
f	fuel
L	liquid injectant
o	free stream
t	total
4	combustor exit conditions

superscripts

'	conditions after normal shock
$\overline{(bar)}$	referenced to ER = 1.0 conditions
*	critical conditions (i.e., conditions where the local speed is equal to the local speed of sound)

I. INTRODUCTION

In the past several years, numerous authors[1,2] have suggested the use of supersonic combustion to extend the operating velocity range of air-breathing propulsion systems or to provide force augmentation for attitude control and lift sustentation for long-range cruise. The application of supersonic combustion to systems which can utilize the potential performance gain is contingent on understanding the phenomena of fuel injection, mixing and heat release in a supersonic flow field, which can be complicated by the presence of shock waves, thick viscous layers, and separated zones. The degree to which the theoretical and semi-empirical solutions utilized in the development of subsonic combustors can be extended or modified for supersonic heat release needs to be demonstrated.

Although numerous articles describing analytical studies of heat addition to supersonic streams have appeared in the literature, very little experimental verification is available. The first work reported in the unclassified literature was begun by Dorsch, et al of NASA in 1955.[3,4,5] Highly reactive fuels such as aluminum borohydride were injected from static ports on a flat plate and on a body of revolution into a cold Mach 2-3 airstream. Oblique shocks were generated from a point upstream of the fuel injection station and a pressure rise which rapidly decayed in the streamwise direction was noted. Optical studies of the flame zone revealed a rather thick low velocity and possibly separated flow region adjacent to the body with sonic and low supersonic flow in the outer portions of the flame.

Dugger and Billig[6] at APL have done somewhat similar work with

pyrophoric fuel injection at or just upstream of the "knee" of various wedge models. Combustion occurring beneath the rearward facing surface acted like a volume source, deflecting the air flowing past the heat addition region. The resultant pressure rise on the aft surface increases lift and decreases drag. If the flow deflection is large, net thrust is produced.

Mention should also be made of the detonation and shock-induced combustion experiments as contrasted to the deflagration combustion tests previously described. Nichols[7] at the University of Michigan and Gross[8] at Fairchild and subsequently Rubins and Rhodes[9] at AEDC have conducted experimental studies of hydrogen combustion with steady, normal and oblique detonation waves. In the former work, a premixed hydrogen-air stream was passed through a supersonic nozzle and discharged into still air. The nozzle pressure ratio was adjusted such that the jet was highly overexpanded, thus creating a strong shock system at the jet exit. The large increase in pressure and temperature across the shock produced favorable conditions for combustion of the hydrogen. In some instances, the combustion was coupled to the shock wave, i.e., steady detonation, and in other tests the presence of the shock wave induced combustion downstream.

Gross and Rubins' technique is to add hydrogen at or downstream of the throat of a Mach 3 nozzle. Opposing wedge surfaces in the test section are situated such that oblique shocks establish a normal shock in the center of the gas stream. Combustion proceeds in the same manner as in Nichols' tests.

The aforementioned experiments have demonstrated the feasibility

of combustion in supersonic streams. The principal difference between these two types of combustion is mixing (and atomization and evaporation in the case of liquid injections).

In deflagration combustion both mixing and kinetics control the rate and extent of heat release since both phenomena occur simultaneously. In detonation combustion, it is generally postulated that the fuel is added sufficiently upstream of the combustion zone so that mixing is virtually completed before the combustion zone is reached. In the mixing zone, the pressure and temperature are so low that the reaction rates are effectively equal to zero. Downstream of the mixing zone, the flow is compressed by an oblique or normal shock wave and the resulting step increases in pressure and temperature greatly increases the reaction rates and combustion proceeds. For most practical situations fuel will be injected into an air stream with mixing and combustion progressively taking place.

The purpose of this thesis has been to acquire a better understanding of deflagration combustion in supersonic streams with the following specific objectives:

1. To demonstrate that fuel could be injected into a supersonic air stream and produce heat release.

2. To develop measuring techniques which would obtain sufficient information to define and explain the observable phenomena.

3. To correlate the experimental results with applicable analyses.

The high combustion efficiency which will be required in flight applications was not expected in these tests, due to less than adequate residence times imposed by facility limitations.

II. DESCRIPTION OF MACH 5 TEST FACILITY AND PYROPHORIC FUEL SYSTEM

The tests were conducted in the Mach 5, ten inch diameter supersonic propulsion tunnel at the Applied Physics Laboratory. Air from high pressure storage vessels is heated in a stainless steel matrix storage heater and supplied to the tunnel plenum chamber at pressures of 90 to 1000 psia and at temperatures up to 2250°R. Running times vary from thirty seconds to five minutes depending on the storage heater capacity and the steam consumption limit on the facility exhauster. The tunnel Reynolds numbers range is from 1×10^6 to 6×10^6 per foot. Figure 1 is a schematic of the test cell layout. The tunnel is an enclosed free-jet type, i.e., the nozzle exhausts into a test cabin and is then recaptured in a converging-diverging diffuser. This type of tunnel has the advantages of having the optical windows located away from the hot jet but has certain inherent difficulties in operating with models of appreciable size. During the testing described herein, models with greater than 19.5% blockage would not operate in the normal mode in which the main tunnel air is ducted to the facility exhauster. However, by switching the exhauster to a nozzle boundary layer bleed and venting the main tunnel air to atmosphere, models as large as 25.5% of the nozzle exit area ran satisfactorily.

The 15" x 15" x 20" test section is equipped with optical quality quartz windows for schlieren observations. All sides of the test section are removable for easy access to the model and instrumentation. The schlieren system is a folded single pass type. The image from the schlieren stop projects onto a multisurfaced prism so that fastax, normal speed and television cameras can be used simultaneously. Direct

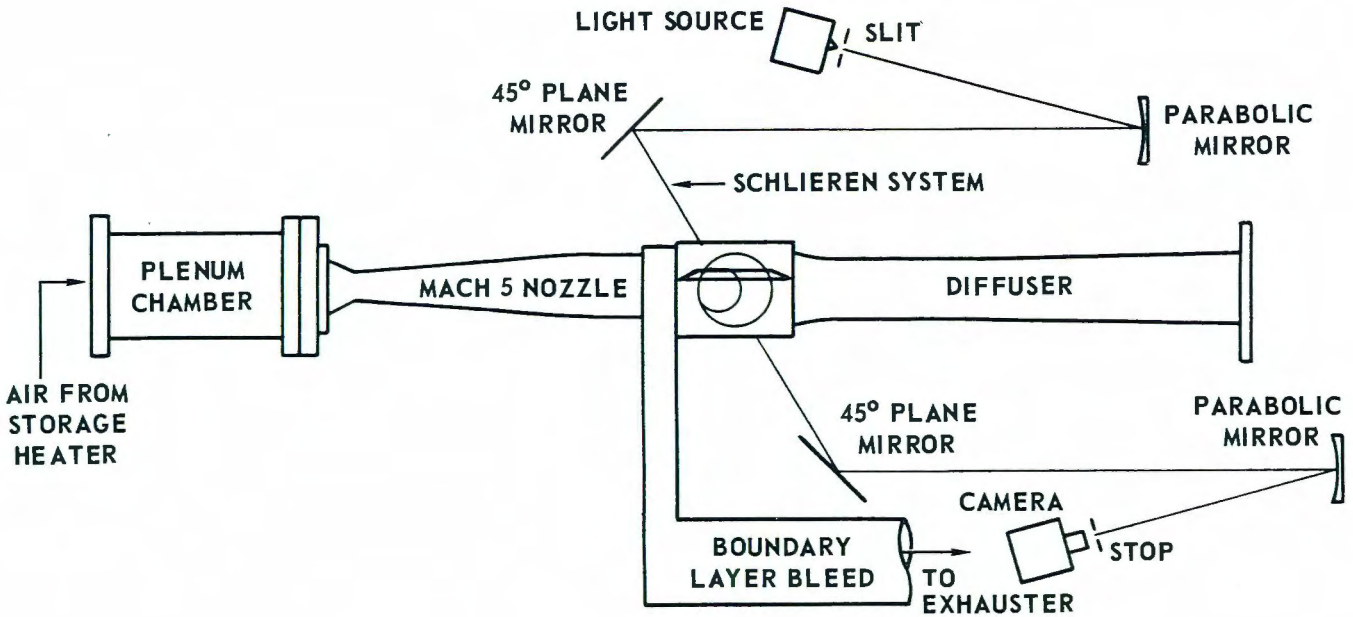

Fig. 1 Schematic Diagram of the Ten-Inch Diameter Mach 5 Tunnel

color motion pictures are also taken during the test runs.

Pressures are measured by either variable inductance or strain gauge type transducers whose output is fed into a 100-channel, 50-channel/second data acquisition system. Output of the data system is then put directly into a Packard Bell 250 digital computer for elementary data reduction (i.e., pressure in psia, etc.) or onto magnetic tape for subsequent data reduction on the main laboratory IBM 7094 computer. Temperatures are measured with thermocouples and outputs handled in a similar manner.

The liquid fuel system is shown in Figure 2. It consists of a dry nitrogen pressurization system, liquid purge, and fuel supply system, fuel heater and flow control. Pyrophoric aluminum alkyl fuels, principally triethyl aluminum were used in these tests. These fuels react with both air and water forming solid aluminum oxide as one of the reaction products. Solids cannot be tolerated in the system as they will clog the fuel injectors. The complete system must be hermetically sealed and all components are isolated from one another by standard valves with teflon packing and seats. In the event that contamination and plugging occur, unaffected components are valved off and the fuel is removed via critically positioned dump valves.

The sequence of operations required to load and use the system are as follows:

1. With all internal valves open dry nitrogen is introduced to the system from the bottle supply and bled from the model fuel manifolds. After sufficient purge time (about five minutes) the final stop valves upstream of the fuel manifolds are closed.

2. The vacuum pumps are started and the dry nitrogen is

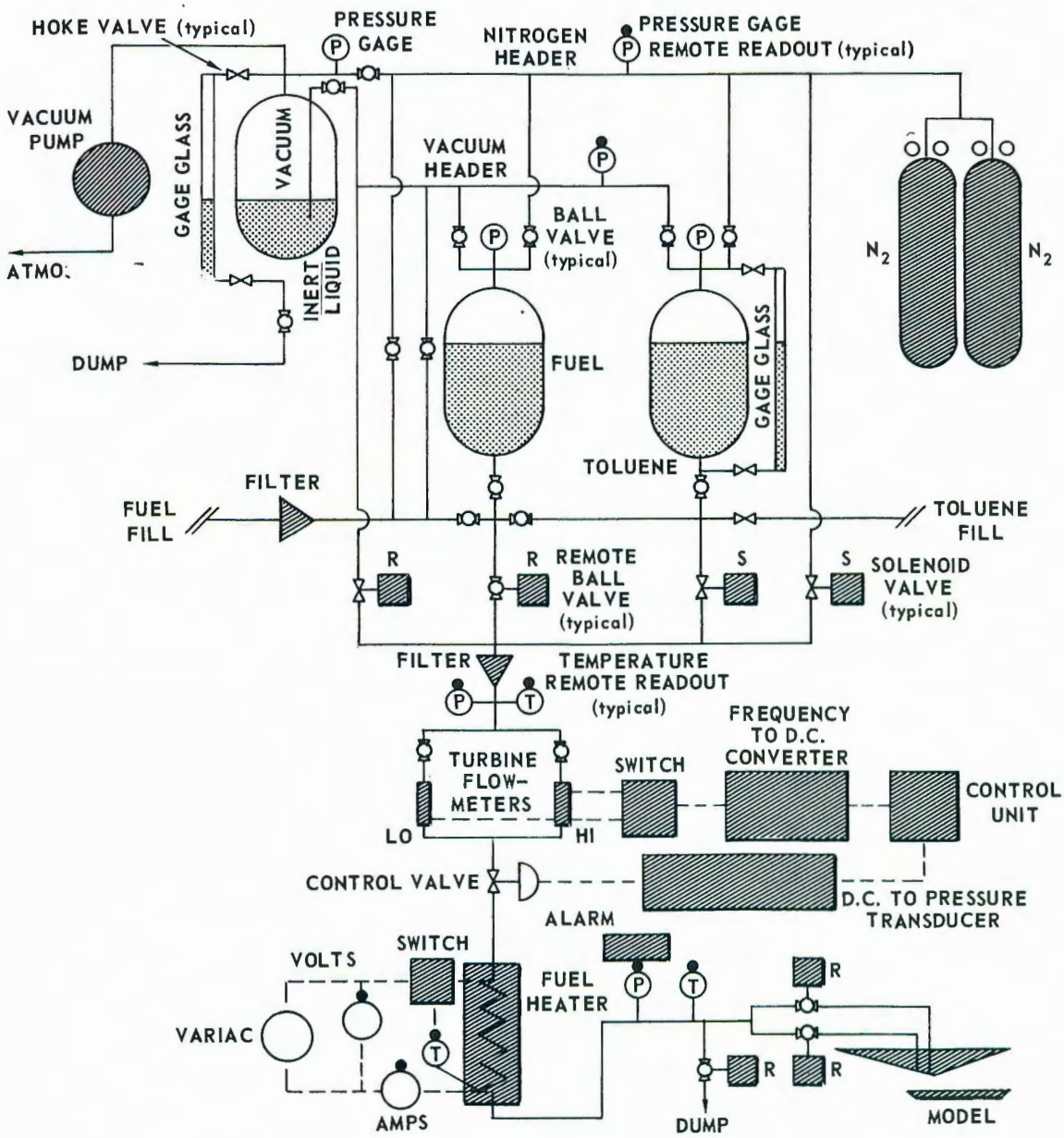

Fig. 2 Schematic Diagram of the Pyrophoric Fuel System

withdrawn from the system until the pressure is reduced to about .1 psia. Dry nitrogen is reintroduced into the system and the pressure is raised to about 250 psia. The nitrogen-bleed-vacuum purge cycle is then repeated. Assuming there is complete mixing of residual air with the dry nitrogen, then each cycle reduces the contaminant concentration by a factor of 2500. Water vapor is eliminated in a similar manner but by a smaller factor per cycle since the saturation point is reached at pressures less than 250 psia. After three cycles, the system is considered oxygen- and water-free.

3. The appropriate valves are closed and fuel from an external source is fed into the reservoir through a 10 micron filter. Dry toluene, which acts as a liquid purge, is then loaded into a reservoir and the system is ready to use.

4. In a typical run, cold flow (no injection) points are taken, followed by a toluene purge flow. The purge removes the air trapped between the last stop valve and the fuel injectors and permits the flow control servo loop and the fuel heater to stabilize. It also provides a test measurement of mass addition effects in the absence of heat addition.

5. The toluene is followed by fuel and data points are taken at various fuel settings and preheat temperatures.

6. Following the burning data, the toluene is reintroduced to flush out the lines, the stop valves are then closed, additional cold flow checks are made, and the test is completed. The final cold flow checks serve the dual function of providing a reference check on the tunnel operating conditions and as a final check on the stability of model pressure instrumentation.

The fuel flow is measured by one of two parallel low and high range turbine flowmeters. Their output is both recorded and simultaneously fed into a servo control loop which converts the frequency output of the flowmeter to a D.C. voltage and compares it with a set-point. The error signal is then fed to a D.C. to pressure transducer which adjusts the pressure on the pneumatically actuated control valve.

A section of stainless steel tubing functioning as the resistance element in a A.C. circuit serves as the fuel heater. Fuel temperature is controlled in a flip-flop manner by sensing the outlet temperature and comparing it with a set-point. Fuel flow can be controlled to within $\pm 1\%$ and fuel temperature to $\pm 5^{\circ}R$.

III. TWO-DIMENSIONAL DUCTED COMBUSTION EXPERIMENTS

The first model tested is schematically depicted in Figure 3. It consists of a 10°-20° half-wedge model with an attached cowl reflector plate. This cowl was positioned such that the wedge compression shock is reflected back to wedge surface at the "knee" of the wedge body. The resulting two-shock compression decelerates the free stream air from Mach 5 to Mach 3.3 behind the second shock. The static pressure was varied from 1.8 to 3.0 psia and the static temperature from 600°R to 700°R in this region, depending upon the free stream conditions. In the absence of fuel injection, the flow would then expand rapidly in the divergent section behind the "knee". The model is four inches in width.

Two transverse rows of fuel ports are located at the "knee" and 3/8 inch upstream on the compression surface. The ports are .031 inch diameter on 0.5 inch centers. The combustor section formed by the expansion (rear) wedge and cowl has a divergence of 20°, which is considerably greater than would be desirable in a realistic combustor duct. The effective area ratio is about three. At a typical average velocity of 4200 ft/sec in the 2.9 inches of length, the air residence time is about 57 microseconds. The calculated fuel residence time is about 40 microseconds greater than the air residence time due to the time required to accelerate the droplets. The velocity of the droplet at the combustor exit is about 90% of the air velocity in spite of the short residence time since the acceleration is about one million "g's".

In the tests, aluminum alkyl fuels were injected from either of the two fuel manifolds at various fuel-air equivalence ratios and fuel temperatures. In general, visual observation indicated that the fuel penetration was about half-way into the supersonic flow (e.g.,

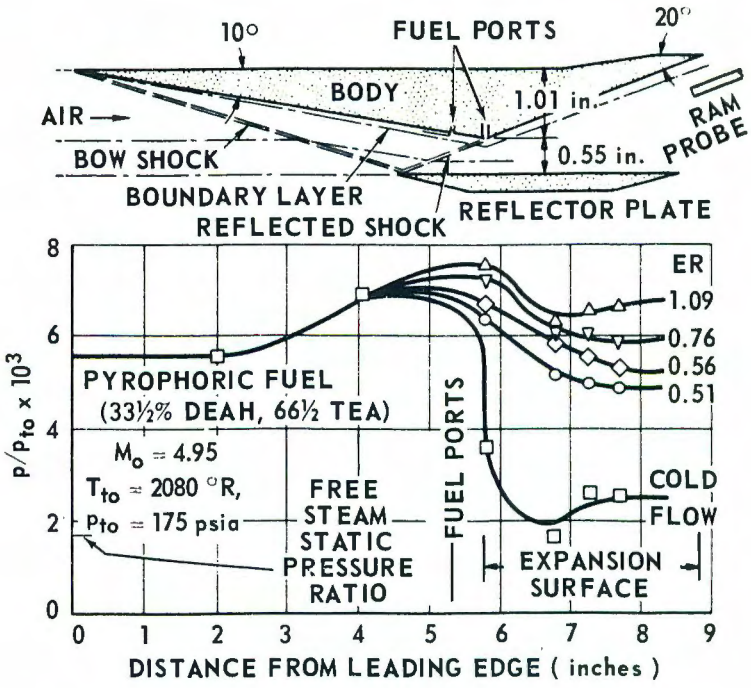

Fig. 3 Schematic of 10°-20° Ducted Combustor and Typical Longitudinal Pressure Profiles

$\sim$ 1/4 inch near the injection station), and visible heat release began less than 0.5 inch from the injection ports. The heat release zone spread to completely fill the duct at the combustor exit. In some tests, burning in the viscous boundary layer ahead of the injection point was noted. A minute quantity of water was injected from a small diameter (.063 inch) tube laying on the surface of the compression wedge and directed downstream toward one jet. Its principal effect was to stabilize combustion at the very low equivalence ratios since the aluminum alkyl fuels are highly reactive with water.

In Figure 3, the experimental pressure profile for a test with a plenum chamber temperature of 2080^{o}R and a plenum pressure of 175 psia is also shown. The data points represent static pressure measurements taken along the centerline of the wedge surfaces. Pressure ratios increase as the fuel-air equivalence ratio (ER) is increased from the lean limit ignition point, ER = 0.51 to ER = 1.09. Transverse pressure distribution for these same runs indicates a slight drop in pressure toward the edges of the model due to edge spillover because the only side plates used were the small structural supports for the cowl.

The static pressure rises slightly in the region of the fuel ports due to rather weak fuel injection shocks. It then drops slightly as it undergoes a small degree of expansion at the "knee" and is then maintained at about a constant level due to continuing heat release in the divergent duct. The average static pressure rise (Δp) in the combustion zone is a measure of the amount of heat released. Figure 4 displays this pressure rise normalized to free stream total pressure, as a function of fuel-air equivalence ratio for all tests on this model. The scatter of the data can be reduced by empirically adjusting

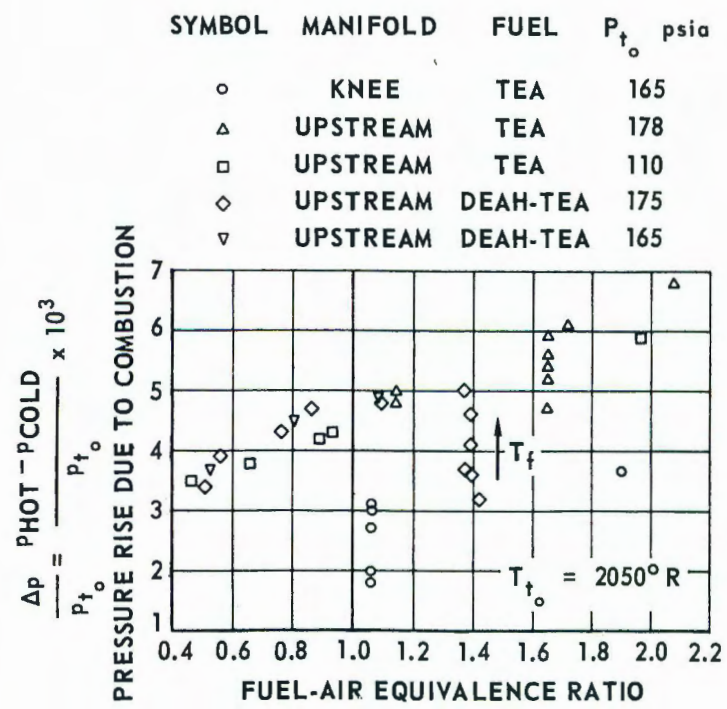

Fig. 4 Pressure Rise Due to Combustion on 10°-20° Ducted Combustor Model

the pressure ratios by the factor

$$.0032e^{\frac{-T_f}{100}}$$

to account for the experimentally observed fuel-preheat-temperature (T_f °F) effect as shown in Figure 5. A complete summary of the test results on this model is given in Table I. The significant results of these tests are:

1. Fuel injection from the upstream injector is more favorable due to longer residence time in the higher pressure and temperature region.

2. There was little difference between the two fuels tested, i.e., triethyl aluminum (TEA), and a 33.5% diethyl aluminum, hydride (DEAH), 66.5% TEA mixture.

3. A small pressure effect might be inferred - the 165-175 psia data were slightly higher than 110 psia data - but it can hardly be termed significant from these data.

4. As indicated by the correlating parameter used on the fuel temperature (T_f), there is considerable advantage to preheating this fuel, TEA, to approximately 250°F, but little change occurs beyond that point.

During the runs pitot pressure measurements were made in the exit plane of the combustor. In most runs, the probe was completely enveloped in the blue-white luminous zone. If it is assumed that there was no pressure gradient normal to the flow direction, then the surface static pressure opposite the probe can be taken as the local static pressure upstream of the probe shock. Static/pitot pressure ratios p/p_t' obtained in this manner can be used to determine the

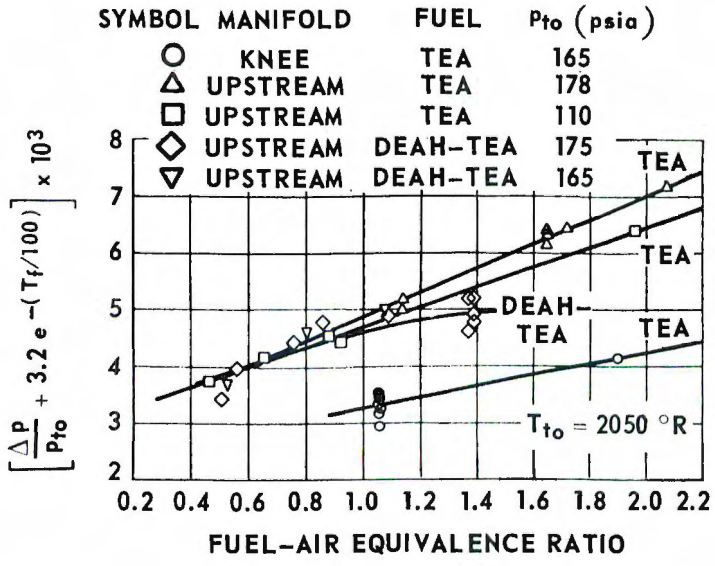

Fig. 5 Normalized Pressure Rise Due to Combustion, Compensated for Injected Fuel Temperature T_f °F on 10°-20° Ducted Combustor Model

TABLE I - SUMMARY OF 10^{o} - 20^{o} DUCTED COMBUSTOR TEST RESULTS

MANIFOLD	FUEL	T_{t_o} (^{o}R)	p_{t_o} (psia)	ER	T_f (^{o}R)	$\frac{\overline{\Delta p}}{p_{t_o}}$	$\frac{\overline{\Delta p}}{p_{t_o}} + .0032e$	$\frac{-T_f}{100}$	M_4
Upstream	TEA	2042	111.1	1.960	189	.0059	.0064		2.44
		2061	110.8	.885	230	.0042	.0045		2.82
		2063	111.0	.655	223	.0038	.0041		2.95
		2071	110.8	.462	263	.0035	.0037		2.98
		2102	111.0	.925	344	.0043	.0044		2.69
Upstream	TEA	2020	178.5	1.650	65	.0047	.0064		2.65
		2029	178.6	1.650	147	.0054	.0061		2.55
		2035	178.7	1.650	181	.0056	.0061		2.57
		2027	178.7	1.650	111	.0052	.0062		2.61
		2036	178.5	1.650	207	.0059	.0063		2.52
		2050	178.3	1.140	287	.0048	.0050		2.68
		2056	178.6	1.140	298	.0050	.0052		2.59
		2064	178.6	1.720	234	.0061	.0064		2.56
		2064	178.5	2.076	222	.0068	.0072		2.37
Upstream	DEAH-TEA	2073	174.9	1.390	74	.0036	.0052		2.92
		2076	174.9	1.370	126	.0037	.0046		2.76

TABLE I - continued

MANIFOLD	FUEL	T_{t_o} (^oR)	p_{t_o} (psia)	ER	T_f (^oR)	$\frac{\overline{\Delta p}}{p_{t_o}}$	$\frac{\overline{\Delta p}}{p_{t_o}} + .0032e^{\frac{-T_f}{100}}$	M_4
Upstream	DEAH-TEA	2077	175.0	1.390	203	.0041	.0045	2.78
		2082	175.2	1.390	238	.0046	.0049	2.70
		2088	175.2	1.370	249	.0050	.0052	2.54
		2091	175.2	1.090	353	.0048	.0049	2.58
		2092	175.4	.860	377	.0047	.0048	2.64
		2096	175.3	.760	316	.0043	.0044	2.71
		2098	175.2	.555	386	.0039	.0040	2.83
		2099	175.2	.506	317	.0034	.0034	2.92
Upstream	DEAH-TEA	2043	165.5	.527	448	.0037	.0037	2.75
		2045	165.3	.803	350	.0045	.0046	2.57
		2049	165.4	1.080	339	.0049	.0050	2.48
Knee	TEA	2099	183.3	1.060	62	.0018	.0035	3.61
		2101	183.6	1.060	81	.0020	.0034	3.38
		2105	183.4	1.060	263	.0027	.0029	3.08
		2117	184.0	1.060	284	.0031	.0033	2.95
		2109	183.7	1.060	305	.0030	.0032	3.03

TABLE I - continued

MANIFOLD	FUEL	T_{t_o} (^{o}R)	p_{t_o} (psia)	ER	T_f (^{o}R)	$\frac{\overline{\Delta p}}{p_{t_o}}$	$\frac{\overline{\Delta p}}{p_{t_o}} + .0032e^{\frac{-T_f}{100}}$	M_4
Knee	TEA	2115	183.4	1.060	309	.0031	.0033	2.94
		2122	183.9	1.900	202	.0037	.0041	2.80

local Mach number. In Appendix A a method of interpreting upstream properties, e.g., combustor exit Mach number from the local static and pitot pressure measurements is developed for a real gas.

An analytical model was developed to see if the observed pressures were consistent with those expected from supersonic heat release. The following assumptions were made:

1. The flow in the plane of the "knee" and the combustor exit is one-dimensional. (A pitot survey in the exit plane showed this to be nearly so.)

2. The pressure in the combustion region is constant and equal to the average wall value. (This simplifies the momentum equation.)

3. The flow isentropically expands from the plane of the "knee" to a new plane which is at the average combustor static pressure. Heat release begins at this plane. The energy equation,

$$h_a + \frac{u_a^2}{2gJ} + f\,(h_f + \frac{u_f^2}{2gJ}) = (1 + f\cdot ER)\,(h_b + \frac{u_b^2}{2gj}), \qquad (2)$$

momentum equation,

$$p_a A_a + \int_a^b p\,dA - \tau_w A_w - p_b A_b = \rho_b A_b u_b^2 - \rho_a A_a u_a^2 - \dot{w}_f u_f \cos\alpha \qquad (3)$$

where α is the injection angle relative to the air stream ($\alpha = 90^\circ$ in this case) and the continuity equation,

$$\rho_a u_a A_a + \dot{w}_f = \rho_b u_b A_b, \qquad (4)$$

equations were solved simultaneously using equilibrium kinetics for TEA-air mixtures. The wall friction term $\tau_w A_w$ was found to be negligible

and was dropped in subsequent calculations. All of the combustor exit flow properties could then be found for any given ER and exit pressure.

The experimentally measured and theoretically computed static pressure vs p/p_t' and Mach number relationships are shown in Figure 6. The abscissa for this figure is the ratio of combustor static pressure (p_4) to free stream stagnation pressure (p_{t_o}). For comparison, a similar relation for an expansion without heat addition is shown. In this case, flow separation or mass addition adjacent to the wall must prevent complete expansion. The large difference between the two theoretical cases results from the significant total pressure loss and Mach number decrease associated with supersonic heat release. The close correlation of data with the constant pressure heat addition theory tends to support the original assumptions and permits a reasonable calculation of the combustion efficiency to be made. For the data points shown, the heat release (under these relatively poor test conditions) only amounted to about 20% of that theoretically available. A complete description of the properties of the aluminum alkyl fuels and a discussion of typical combustion conditions is given in Appendix B. A definition of combustion efficiency as related to these tests is also included in this section.

The second model tested is shown in Figure 7. This model differs from the first in that the combustor divergence has been reduced from 20° to 10° and the combustor length correspondingly increased from 2.9 to 5.7 inches. As in the previously tested model, the triethyl aluminum fuel was injected through a transverse row of 0.031 inch diameter holes spaced 0.5 inch on center and located 3/8 inch upstream of the "knee" of the wedge surface. In Figure 8, the longitudinal

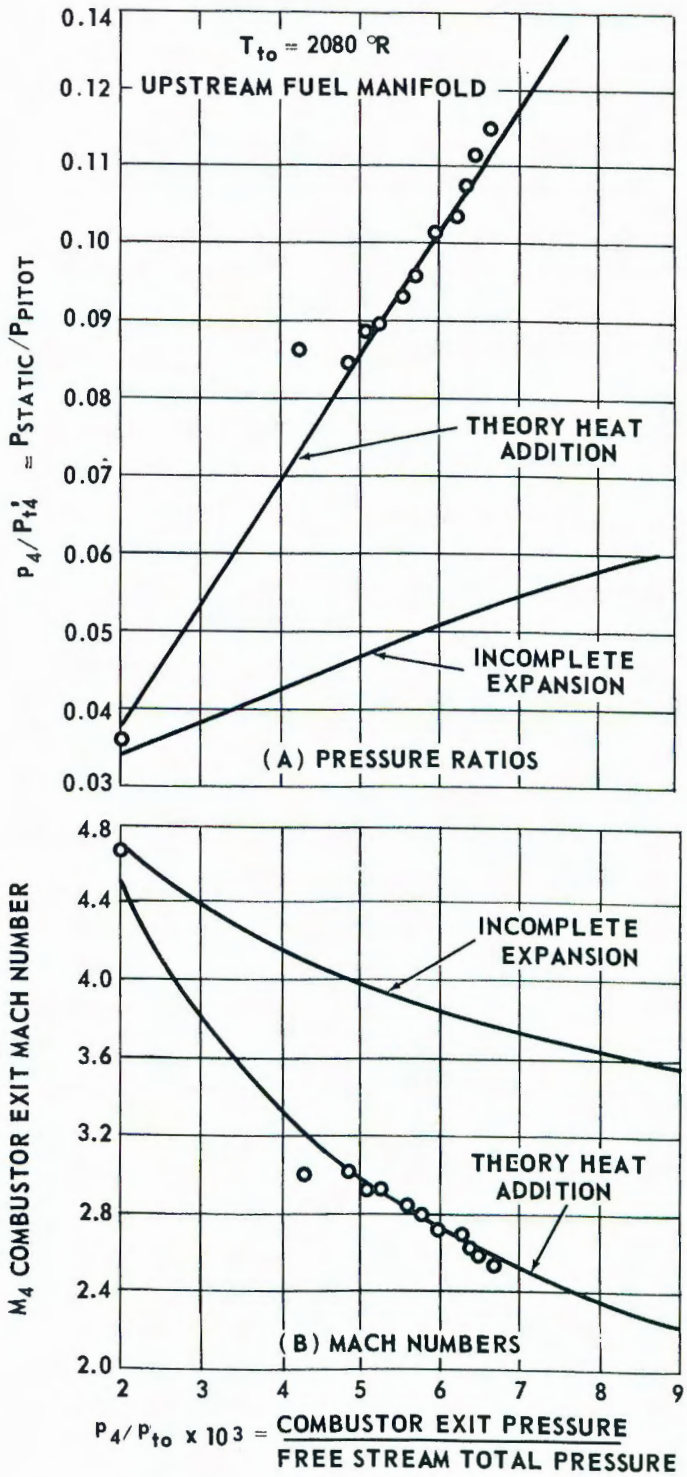

Fig. 6 Combustor Exit Pressure Ratio and Mach Number as Function of Exit Pressure for 10°-20° Ducted Combustor

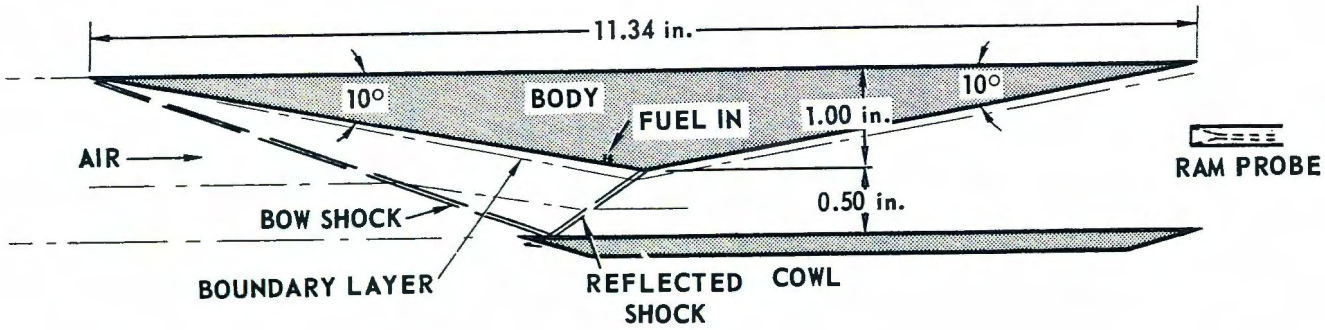

Fig. 7 Sketch of 10°-10° Ducted Combustor Model

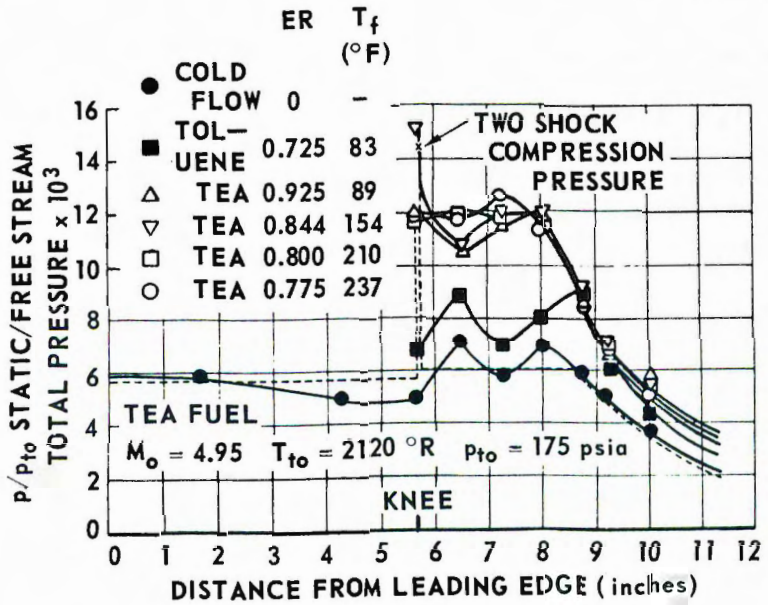

Fig. 8 Typical Longitudinal Pressure Profiles from 10°-10° Ducted Combustor Test

pressure profile is shown. The two-shock compression produces a static pressure of 2.50 psia and static temperature of 595°R at Mach 3.24 in the plane of the "knee". However, since the second shock strikes the body very near the "knee", and combustor divergence begins at the same point, there is no appreciable body area upon which this maximum pressure can act. Prandtl-Meyer turning at the "knee" therefore drops the pressure to the theoretical level shown by the dashed curve for cold flow. At a point about halfway back in the diverging section, two-dimensional effects from cross-flow expansion (and side spillover) begin to affect the pressures seen by the body-centerline pressure ports, and a near-isentropic-expansion pressure decay is seen.

When fuel is injected just ahead of the "knee", the heat release tends to counteract the Prandtl-Meyer expansion and to hold the pressure nearer the two-shock compression level. The data in Figure 8 show that for any given combination of fuel flow rate and fuel preheat temperature represented by one of the runs, heat release must have occurred continuously and at nearly constant pressure for half the duct length, but the heat release rate was insufficient thereafter to also counteract the cross-flow expansion effect and consequent pressure decay. Fuel temperatures in these tests varied about inversely with fuel flow rate since the preheater was not controlled. The small differences in the burning pressure traces for the four runs indicate that the two effects nearly compensate one another.

Pitot traverses were again made in the exit plane and the previously described theoretical analysis was modified to account for the non-constant combustion pressure. The magnitude of the $\int_a^b pdA$

term in the momentum equation (3) must be determined to solve the set of equations. This added complexity was handled by using the wedge surface static pressure distribution and making a summation over the projected area in the streamwise direction. Mass addition in the absence of heat addition solutions were also generated. Figure 9 shows the comparison of data with theory. The abscissa for this figure is the ratio of exit static pressure (p_4) to free stream stagnation pressure (p_{t_o}). The ordinate for the upper set is the static/pitot pressure ratio at the exit, from which the exit Mach number M_4 was calculated for the lower set.

Since the model has no side plates, some side spillover (cross-flow expansion) is expected, and it should increase with increasing pressure rise in the combustor. The data show this trend. Theoretical curves for 10% spillover (due to a hypothetical 10% increase in effective flow area by the time the exit plane is reached) were added to Figure 9. The highest fuel flow rate did produce a result near this 10% spill curve. The calculated combustion efficiency is about 25% of theoretical, slightly higher than in the 10^{o}-20^{o} combustor tests. Points are also shown for the toluene purge liquid, which does not burn at these conditions but produces a small mass addition effect.

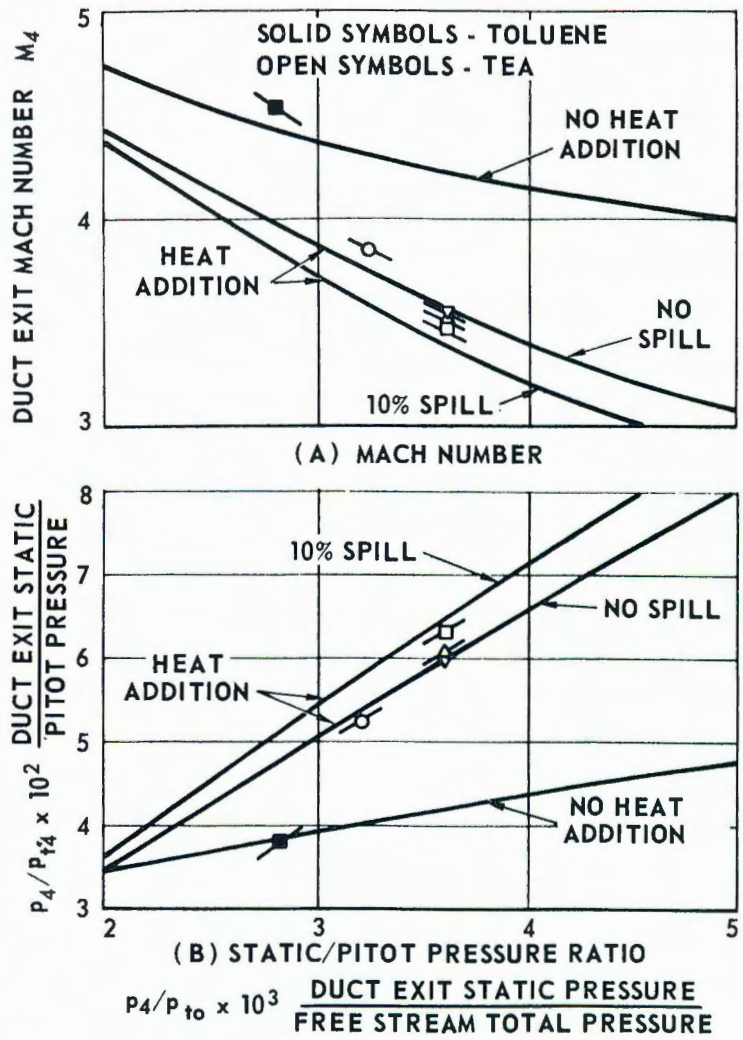

Fig. 9 Comparison of Theory with Experimental Data for 10°-10° Ducted Combustor Test

IV. FLAT PLATE COMBUSTOR ANALYSIS

The use of lateral jets for side force attitude control and in nozzles for thrust vector control has received considerable attention.[10,11] If a reactive injectant could be utilized, the favorable aerodynamic interference effects would be further augmented by supersonic heat release. The model depicted in Figure 10 was used to estimate the performance of "external burning" on a flat plate in supersonic flow.

Fuel is injected near the leading edge, causing a separated-flow region and a corresponding oblique injection shock. The fuel penetrates to a height Y_1 and combustion begins in the plane labeled Y_2 and is completed at plane Y_3. For additional simplicity, the heat release is assumed to proceed at a rate to maintain the pressure level attained by the injection separation. Thus, the injection shock is represented by a straight line until point C is reached, where expansion commences. At point D in the Y_3 plane, expansion begins in the combustion gas, as represented by the "leading Mach lines", DE. Pressure is therefore assumed to be constant throughout the region ABDE. To avoid the complex characteristic solution of the flow field of the combustion gases, the surface pressure in the expansion region (EF) is assumed to be the arithmetic mean of combustion and free stream pressures. Equilibrium combustion of triethyl aluminum in air with 100% combustion efficiency using the procedure developed by Browne and Williams[12] was carried out on a high speed computer. No heat or mass transfers across the hot-cold interface.

The normal force specific impulse is defined as the total force resulting from pressure above ambient divided by the fuel flow

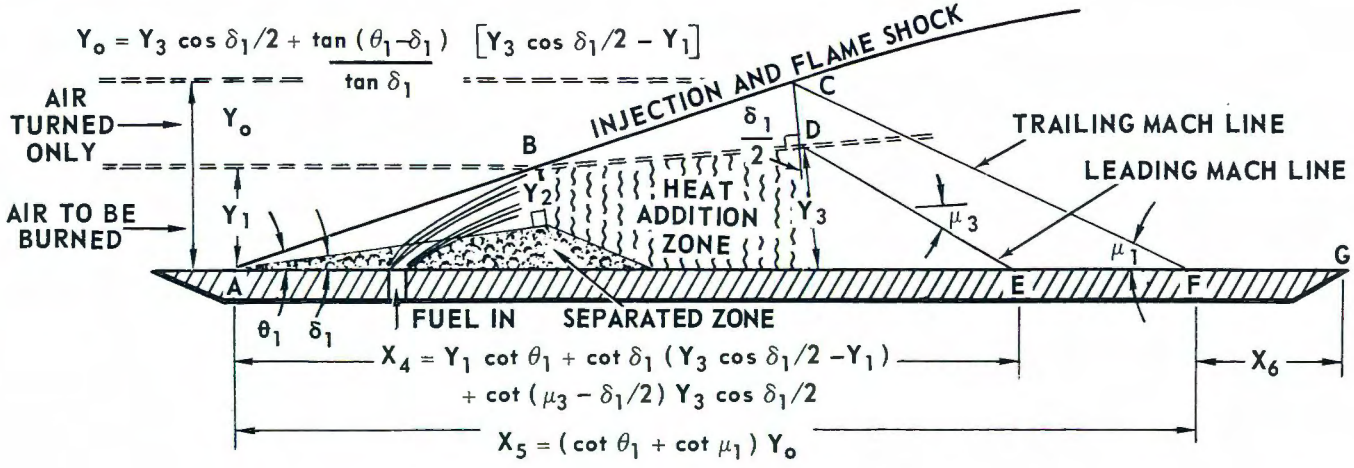

Fig. 10 Theoretical Model of Constant Pressure Heat Addition on a Flat Plate

rate.

$$I_{sp} = \frac{F_N}{\dot{w}_f} = \frac{(p_2 - p_o)\left(\frac{X_4}{Y_1} + \frac{X_5}{Y_1}\right)}{2f\ ER\ \rho_o\ u_o} \tag{5}$$

The normal force coefficient is the total side force divided by the product of the area subjected to pressure above ambient and free stream dynamic pressure.

$$C_N = \frac{F_N}{q_o A} = \frac{(p_2 - p_o)\left(\frac{X_4}{X_5} + 1\right)}{2q_o} \tag{6}$$

Table II summarizes the computer results for cases having a range of free stream, Mach numbers, altitudes, equivalence ratios and injection shock strengths. Cases labeled with asterisks have injection shock strengths and pressure ratios which correspond to separation of a turbulent boundary layer as predicted by Mager.[13] Experiments with non-reactive injection[14,15] have resulted in reasonable verification of the average pressure as estimated by Mager. In the following discussion of experiments of triethyl aluminum injection onto a flat plate at Mach 5, the injection shock was somewhat weaker and separation was apparent. Changes in the geometry of the fuel injector may permit control of the injection shock strength so that all of the cases listed can be of interest. The cases studied were limited to those in which the Mach number at the end of combustion was supersonic; however, subsonic solutions are possible and may in fact be desirable at low Mach numbers.

In Figure 11 the normal force specific impulse and force coefficient dependence on Mach numbers is shown for equivalence ratios of 1.0 and 0.25 at 35,000 ft altitude. For lean mixtures the specific

TABLE II - FLAT PLATE EXTERNAL BURNING PERFORMANCE PARAMETERS

Mach	Z K ft	δ_1 deg	θ_1 deg	ER	Y_0/Y_1	Y_2/Y_1	Y_3/Y_1	X_5/Y_1	μ_3 deg	I_{sp} sec	C_N	$\bar{I}_{sp}$ sec	$\bar{C}_N$
3	35	5	23.16	.50	23.17	.793	5.673	119.6	68.63	7344	.0536		
"	"	"	"	.25	12.44	"	3.411	64.3	47.09	8058	.0548		
"	"	*14	31.25	.25	3.45	.572	2.105	15.4	53.85	7044	.2060		
4	35	*12.5	24.59	1.0	7.88	.503	4.534	47.7	65.84	4776	.1312	4776	.1312
5	35	5	15.09	1.0	19.83	.673	7.213	170.6	43.54	5574	.0342	5574	.0342
"	"	"	"	.75	16.69	"	6.177	143.6	39.78	6288	.0344	5294	.0290
"	"	"	"	.50	11.89	"	4.593	102.3	33.80	6798	.0348	4076	.0209
"	"	"	"	.25	6.38	"	2.776	54.9	26.02	7502	.0358	2414	.0115
5	0	*10.5	19.81	1.0	5.45	.477	3.375	41.8	39.36	3718	.0932	3718	.0932
"	35	* "	19.86	1.0	17.53	.479	4.266	54.7	45.58	4786	.0917	4786	.0917
"	"	* "	"	.75	14.25	"	3.655	45.8	41.57	5408	.0928	4526	.0777
"	"	* "	"	.50	9.32	"	2.738	32.7	35.38	5918	.0949	3534	.0567
"	"	* "	"	.25	3.68	"	1.688	17.5	27.44	6722	.1005	2158	.0323
"	82.3	* "	"	1.0	6.94	"	4.161	53.2	44.97	4662	.0919	4662	.0919
"	35	15	24.31	1.0	4.16	.393	2.988	29.6	47.94	4388	.1554	4388	.1554
"	35	20	29.75	1.0	2.67	.341	2.167	17.7	51.73	4106	.2427	4106	.2427
6	35	* 9	16.65	1.0	6.76	.328	4.127	62.5	36.08	4776	.0667	4776	.0667
8	35	5	10.86	1.0	10.49	.542	5.373	137.9	25.70	5178	.0246	5178	.0246
"	"	* 6.5	12.17	1.0	7.13	.469	7.283	89.6	25.94	4874	.0356	4874	.0356

TABLE II - continued

Mach	Z K ft	δ_1 deg	θ_1 deg	ER	Y_0/Y_1	Y_2/Y_1	Y_3/Y_1	X_5/Y_1	μ_3 deg	I_{sp} sec	C_N	$\bar{I}_{sp}$ sec	$\bar{C}_N$
8	35	* 6.5	12.17	.75	6.01	.469	3.685	75.6	24.02	5534	.0360	4666	.0304
"	"	* "	"	.50	4.30	"	2.769	54.1	20.84	6070	.0368	3666	.0222
"	"	* "	"	.25	2.31	"	1.704	29.1	16.42	6896	.0389	2234	.0126
"	"	10	15.52	1.0	3.60	.359	2.688	41.5	26.60	4374	.0690	4374	.0690
"	"	20	26.43	1.0	1.09	.252	1.083	10.8	29.75	3742	.2265	3742	.2265
10	35	* 5	9.54	1.0	7.65	.477	4.497	121.7	20.51	5008	.0216	5008	.0216
"	35	10	14.86	1.0	2.47	.309	2.029	34.2	21.26	4202	.0644	4202	.0644

* Turbulent separation deflection

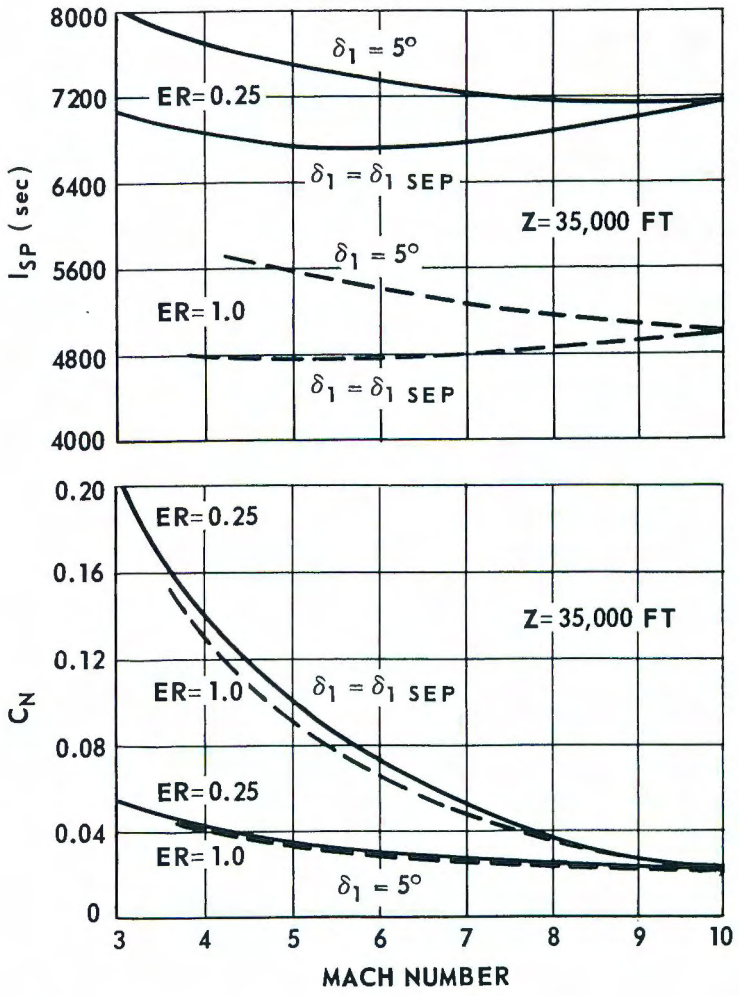

Fig. 11 Normal Force Coefficients and Specific Impulses for a Flat Plate with Constant Pressure Combustion of TEA Fuel

impulse is about 2000 seconds higher. For deflections equal to the above defined separation, $\delta_1 = \delta_{1\ sep}$, the impulse is essentially invarient with Mach number. Even for cases of constant $\delta_1 = 5^o$, the impulse dependence on the Mach number is small, decreasing monotonically with increasing M_o. The normal force coefficient C_N is mainly dependent on deflection angle, increasing only slightly with lower ER. As for most aerodynamic surfaces, larger deflection results in greater force coefficients.

Figures 12a and b show the equivalence ratio ER and deflection effects on I_{sp} more clearly for cases in which all other parameters are held constant. Figure 12c shows the altitude effect at $M_o = 5$, $\delta_1 = \delta_{1\ sep}$. At constant M_o (but varying u_o), temperature rather than pressure has the dominant effect on specific impulse, which is shown by the rapid rise in impulse from sea level to the tropopause and correspondingly slight decline in the constant-temperature, decreasing-pressure region. Of course, if a comparison were made on a constant velocity basis (say, 5000 ft/sec), the effect of altitude would be smaller (but deflection angles would have to be adjusted for M_o variation). ICAO standard day air properties were used throughout.

The results of the theoretical study are dimensionless with regard to the geometric variables. For flight models certain constraints will bound the range of practical geometries. Two principal limitations will be a minimum practical combustor length for efficient combustion and a maximum height of fuel jet penetration. The latter effect is more pronounced for low equivalence ratios since low ER requires relatively greater jet penetration. This effect is dramatically shown in Table II. The last two columns $\overline{I}_{sp}$ and $\overline{C}_N$ are the impulse and force coefficients

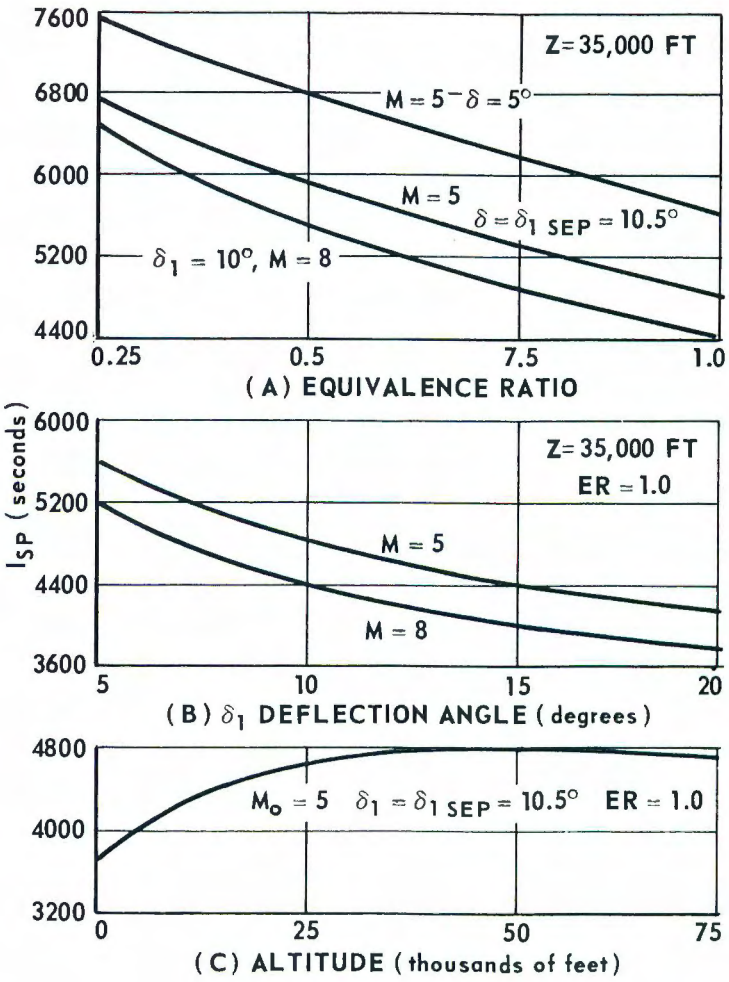

Fig. 12 Normal Force Specific Impulse as Function of Equivalence Ratio, Deflection Angle, and Altitude for Flat Plate at Mach 5 with Constant Pressure Combustion of TEA Fuel

which would result for equal fuel penetration depths Y_1 for cases with the same M, Z, and δ_1 and the same total length but different ER ($Y_1 = Y_{1\ @\ ER\ =\ 1}$). In effect, this constraint forces the expansion to be completed before the end of the plate is reached for ER less than 1.0. The flow model would be lengthened by the distance X_6 (Figure 10) with zero pressure coefficient, hence lower net impulse and force coefficients. The net result reverses the trend of better performance for lower ER and instead shows the desirability of rich operation if penetration rather than length is controlling.

The above theoretical treatments can be applied directly to planar surfaces at other than zero incidence to the free stream. It can also be readily modified to handle single-port rather than multi-port or line-source injection by using half-conical flow surfaces and deflection surfaces rather than two-dimensional ones.

V. FLAT PLATE EXPERIMENTS AT MACH 5

A photograph of the experimental model is shown in Figure 13. Figure 14 is a schematic illustration of this model. It is a water-cooled plate 6 inches wide, 15 inches long and 1.25 inches thick, with a removable leading edge. The model has three drilled-hole fuel manifolds, plugged at each end and fed from the center. Fuel ports are again 0.031 inch diameter holes drilled normal to the manifold on 0.5 inch centers. Three removable fuel-injector plugs are located 4.5 inches from the leading edge. Thirty-five static pressure taps are positioned throughout the surface so that complete pressure surveys can be taken along the model and transversely across the model at four stations. Thermocouples are located at five places on the surface and in each of the fuel manifolds. A traversing pitot tube is located 10.25 inches from the leading edge on the model centerline for ram pressure measurements.

In the test described, the Mach number in the flow field ahead of the fuel injection shock was 5.04. The static pressure was 0.78 psia and the static temperature was 345^{o}R.

Figure 15 shows static pressure profiles taken along the model centerline for "cold" flow (no injection) and for toluene and triethyl aluminum (TEA) fuel injection from the forward fuel manifold. The rather abrupt pressure rise 2.5 inches from the leading edge followed by a decay back to about the free stream level in the toluene curve is as expected for non-reacting liquid injection. Schlieren observations of the flow field confirmed this result.

With TEA injection the pressure first rises, then decays slightly due to the injection shock followed by weak expansion waves,

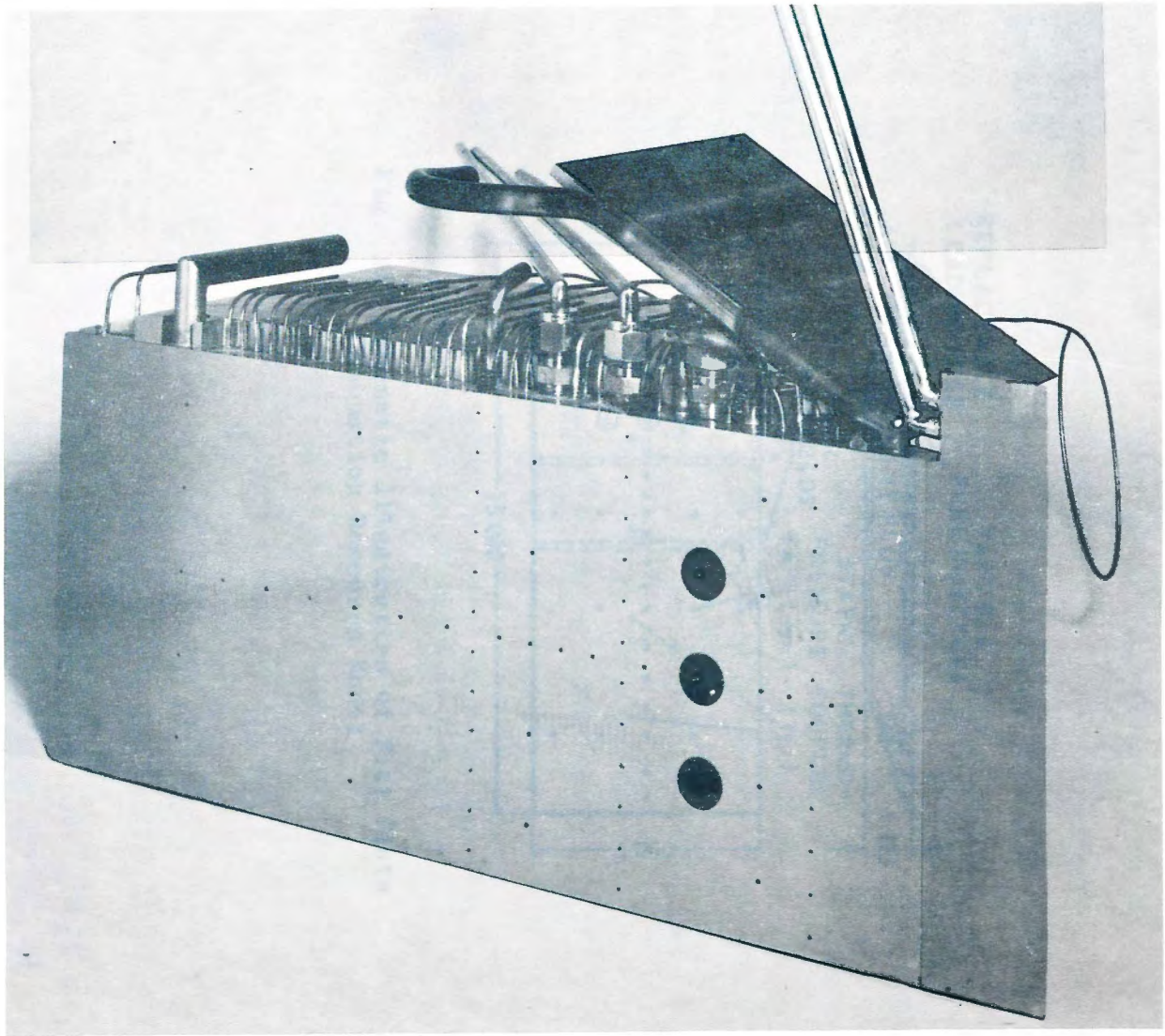

Fig. 13 Flat Plate Combustion Research Model

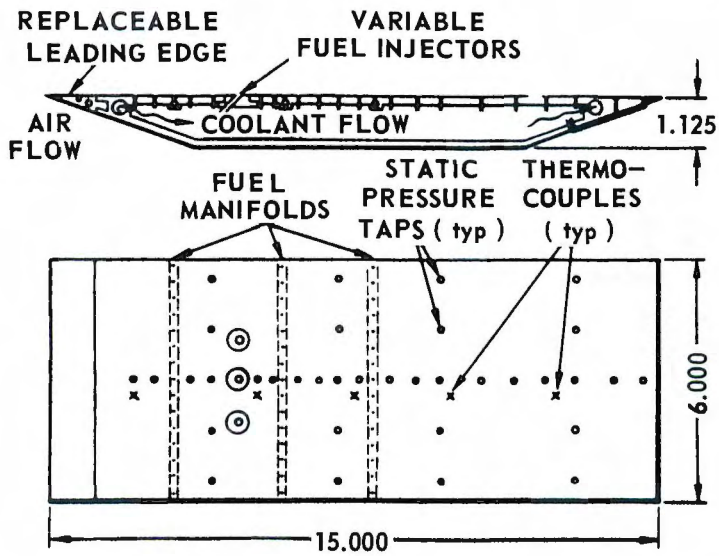

Fig. 14 Schematic Illustration of Flat Plate Combustion Research Model

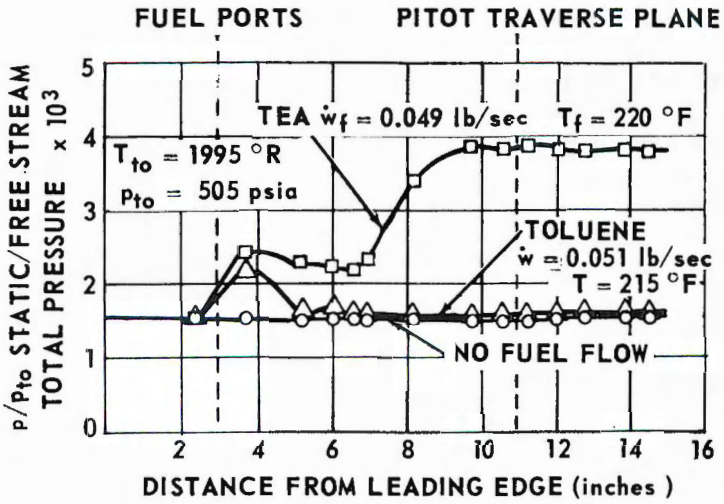

Fig. 15 Longitudinal Pressure Profiles from Flat Plate Combustor Test at Mach 5.04

and then rises to a near constant value as the heat release starts to take place. The continuing relatively constant pressure plateau to the trailing wedge indicates that heat release is continuing and has not been completed in the 12 inches.

In order to appraise the latter situation, a study of droplet evaporation was undertaken. The technique proposed by Zwick, Grubman and Hardy[16] was used to determine the droplet diameter as a function of time. A necessary input for this calculation is the initial droplet diameter. The empirical relationship of Ingebo and Foster[17]

$$d_0 = 3.9 \left[\frac{\sigma_L \mu_L}{\rho_g \rho_L (u_g^3)} \right]^{0.25} (d_j)^{0.5} \qquad (7)$$

was used to determine the volume mean initial drop diameter. For the TEA flow rate of .047 lb/sec at 230°F the calculated d_0 is $.290 \times 10^{-4}$ ft, or about 9 microns.

To calculate the droplet trajectory the analysis by Zwick, et al[16] had to be modified to account for the observed combustion phenomena. In their analysis, it was assumed that the droplet is accelerated by an air stream parallel to the plate and therefore the fuel penetration is dependent only on its initial momentum and the ratio of injection and free stream velocities. The penetration resulting from this type of calculation would be but a small fraction of an inch at the trailing edge. This is contrary to the observed wedge-shaped luminous region extending from the surface at two inches aft of the injection station to about 1.8 inches from the plate at the trailing edge.

Greater fuel penetration can be postulated in the following

way. The fuel penetrates through the separated region with no effective downstream displacement (in fact, some fuel can recirculate upstream and burn in the separated boundary layer[6]), at which point it encounters an airstream moving not parallel to the plate but away from the surface at an inclination determined by the injection-separation shock strength. The air stream accelerates the droplet both downstream and away from the plate. Subsequent turning of the air stream due to the expansion and recompression by the flame shock similarly affects the droplet. Once the flame shock is crossed, the direction of the main stream is dependent on the distance from the plate according to the postulated constant pressure heat addition model. The stream moves parallel to the plate near the surface but in the direction of the main stream deflection along the hot-cold interface.

Three calculated droplet trajectories are shown in Figure 16. The lowest curve represents a calculation according to the technique by Zwick, et al.[16] The two upper curves were determined according to the above-described modification of that theory. In the trajectory with the greatest penetration the droplet is assumed to be near the hot-cold interface. In the other case, it is assumed to be near the center of the heat addition zone. These curves accordingly diverge 4.75 inches downstream of the injection point where they enter the flame zone. For reference, both the observable luminous zone and the position of the boundary of heat release as deduced from pitot pressure measurements are shown.

In order to analyze the pitot pressure measurements, it is necessary to postulate a more applicable flow model than that of Figure 10, since combustion is displaced a slight distance downstream

A. OBSERVED LUMINOUS BOUNDARY
B. HEAT ZONE BOUNDARY FROM PITOT MEASUREMENT
C. TRAJECTORY BASED ON INTERFACE DEFLECTION
D. TRAJECTORY BASED ON CENTERLINE DEFLECTION
E. TRAJECTORY BASED ON NO NORMAL ACCELERATION

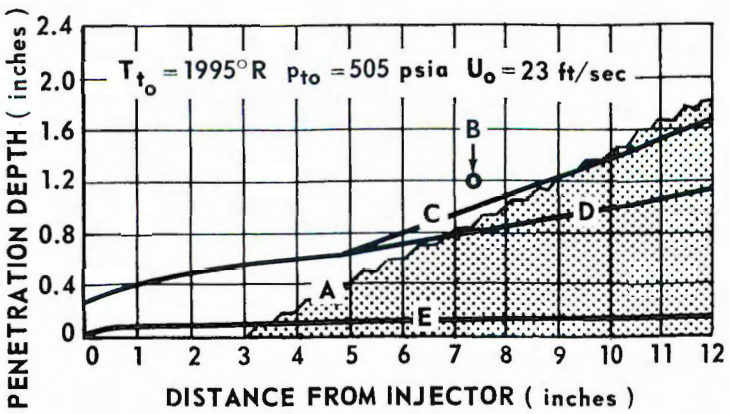

Fig. 16 Calculated Droplet Trajectories for TEA Fuel Injected into a Mach 5.04 Airstream

and is only partially completed. A viscous layer is also present. Figure 17 shows the concept of the flow picture.

In this model the incoming air is divided into three major streamtubes: boundary layer air, inviscid burned air, and air that is turned but not burned. The typical Mach number profile indicates that the properties are not uniform in the major streamtubes as in the case of the ducted wedge tests. Thus, for detailed analysis, the streamtubes must be further subdivided or suitable integrations of properties must be made to reduce the problem to a one-dimensional analysis. The major streamtube boundaries are determined in the following manner: The height of the boundary layer streamtube at the injection shock h_1 is determined by a cold flow pitot pressure traverse and checked with a calculated boundary layer thickness. This calculation also provides an estimate for the total mass flow in the streamtube before fuel injection. After fuel injection it is assumed that no further inflow into the boundary layer occurs and the increase in h_4 above h_1 is due to heat release and additional viscous losses. The downstream pitot traverse determines h_6 and the sum of h_5 and h_4. Since the flow in the outside streamtube is inviscid and adiabatic, the upstream height h_3 can be specified by solving wedge-flow relationships consistent with observed shock waves and pressure measurements. The difference between the total height of the three streamtubes and $h_1 + h_3$ determines h_2. Assuming that the injected fuel is proportionally divided on a mass basis between the two major heat release streamtubes, then all of the necessary conditions are now specified to analyze the combustion except the $\int pda$ term in the momentum equation for each streamtube. This integral is the product of the local pressure and the incremental

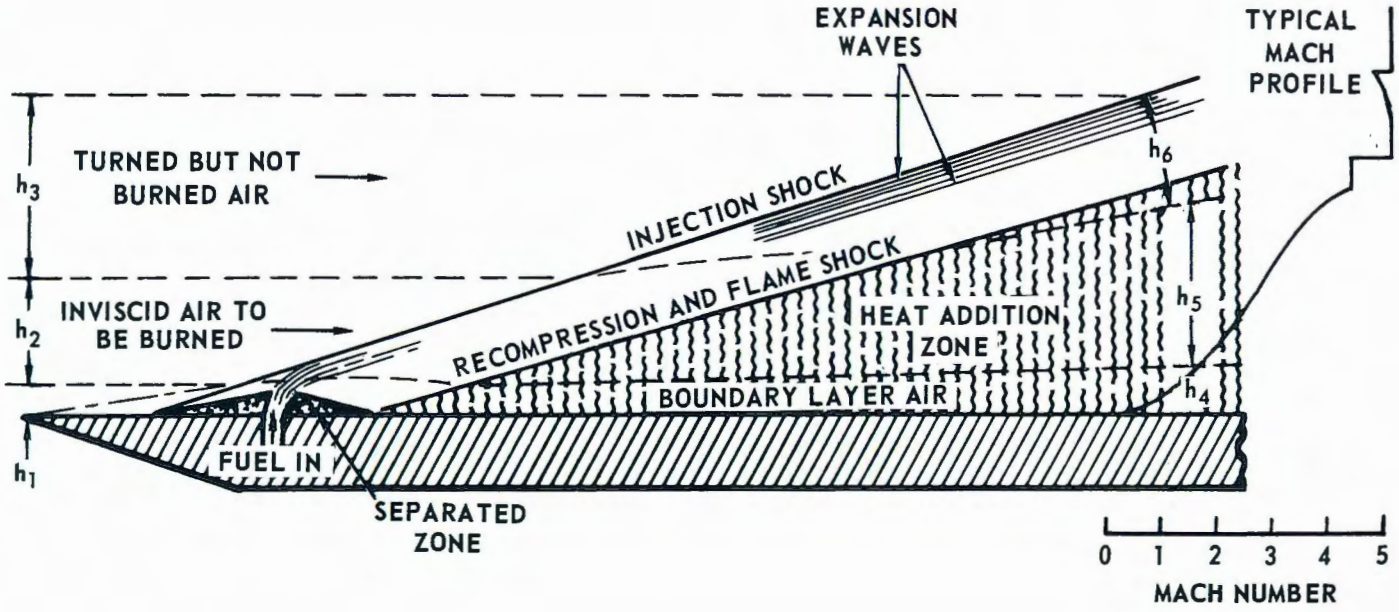

Fig. 17 Experimental Flat Plate Combustor Flow Model

projected area in the flow direction summed over the streamtube boundaries (Eq. 3). As a first approximation, if the wall static pressure is assumed to be constant in planes normal to the surface, a further refinement can be made by analyzing schlieren pictures of the flow field and actually positioning the shock waves. If the Mach profile across h_5 is relatively flat, then the center streamtube is now analogous to the ducted wedge case. In this circumstance, the pressure-area integral term in Eq. 3 is satisfied by assuming the wall static pressure on the plate side of the streamtube and using the wedge flow pressures on the outer side.

For the data point shown, the TEA fuel flow rate was .049 lb/sec. The pitot profile measurements showed $h_5 + h_4 = 1.20$ inches. The calculated upstream heights were $h_1 = .05$ inches, $h_2 = .61$ inches, and $h_3 = 1.93$ inches. At the traversing plane, which was 7.3 inches downstream of the injection port, the calculated average combustion efficiency was 31.5%. The average equivalence ratio in the combustion zone was almost 1.0.

It is possible to relate the experimental result to the more elementary of the theoretical models. For the calculated capture height Y_1 and the measure pressure ratio of .0038/.0015 = 2.53 at Mach 5.04, the theoretical length of the constant pressure region X_4 is 31.0 inches and the total length is 62.4 inches. Combustion would be completed 24 inches from the leading edge and the resulting specific impulse would be 5760 sec. An integration of the pressure rise in the test reported gives a normal force specific impulse of 1350 sec.

VI. SUMMARY AND CONCLUSIONS

Chemical heat release has been observed when highly reactive fuels are injected into supersonic streams. For the relatively small models and modest test conditions reported the combustion efficiency is low due to less than adequate fuel residence times. Simple round orifices served as fuel injectors and provided calculated initial droplet diameters of about 10 microns, which were too large to completely evaporate in the tested combustor length. Optimization of the injector design and/or longer combustors is required to improve efficiency. Factors such as the fuel preheat temperature can have a pronounced effect on performance.

The use of one-dimensional equations to describe the flow measurements is possible in some cases but cannot be adopted a priori as evidenced in the flat plate test results. However, suitable adjustments can be made in a two-dimensional flow field which will reduce it to a psuedo-one-dimensional flow, thus permitting relatively simple evaluation. In either situation, the importance of an accurate pitot pressure survey is clearly evident. When pitot measurements are made in supersonic flow it is necessary to account for the change in properties across the normal shock produced by the probe. Since the classical Rankine-Hugoniot and Raleigh pitot formulae are not directly applicable for real gas combustion products a suitable correction factor is needed. This factor is developed in the Appendix.

Theoretically determined side force specific impulses based on constant pressure combustion adjacent to a flat plate indicate that large gains are possible compared to the impulses that can be achieved with the non-reactive injectants. The flat plate experiments showed that for at least these particular test conditions constant pressure heat addition

is possible, but only after a finite ignition delay period.

VII. APPENDIX A

USE OF PITOT PRESSURE MEASUREMENT FOR DETERMINING COMBUSTOR EXIT PROPERTIES

The principal difference in the evaluation of performance from test measurements of supersonic combustors as contrasted to subsonic combustors is the absence of a defined sonic point. The subsonic combustor is invariably connected to a converging-diverging nozzle in which the Mach number must equal one at the minimum cross-sectional area. Therefore, it is only necessary to measure one additional property at this point in the flow to determine combustor performance assuming the inlet conditions are defined. Generally, the measured property is either the static or total pressure. In the supersonic combustor the flow will usually be supersonic throughout and the Mach number is not known a priori at any downstream station, therefore an additional measurement is required. The two most practical property measurements are the static and pitot pressures, since other properties such as velocity, temperature or density are extremely difficult to measure with an acceptable degree of accuracy. In supersonic flow there is, of course, a normal shock in front of a pitot probe and the probe reads ram rather than total pressure. At low temperatures this presents no difficulty since the well known Rayleigh Pitot Formula[18]

$$\frac{p_{t_o}}{p_o} = \frac{\left[\left(\frac{\gamma + 1}{2}\right) M_o^2\right]^{\frac{1}{\gamma - 1}}}{\left[\left(\frac{2\gamma}{\gamma - 1}\right) M_o^2 - \frac{\gamma - 1}{\gamma + 1}\right]^{\frac{1}{\gamma - 1}}} \qquad \text{(i)}$$

adequately describes the relationship between the pitot pressure and properties upstream of the probe normal shock.

At elevated stagnation temperatures the temperature rise across a normal shock is considerable and since γ is a function of temperature, it also changes. Equation (i) is no longer strictly correct unless for each particular set of flow conditions an average γ can be found which will satisfy the relationship. Rather than introduce this complexity, it is more reasonable to explore property relationships which are only weakly dependent on γ.

For hypersonic flow the relationship[19]

$$\frac{p_t'}{p_o} \approx 1 + 2\frac{q_o}{p_o}\left(1 - \frac{1}{2}\frac{\rho_o}{\rho'}\right) \qquad \text{(ii)}$$

where

$$\frac{\rho_o}{\rho'} = \frac{a_o^{*2}}{u_o^2} \qquad \text{(iii)}$$

is accurate to about 1% or less for Mach numbers greater than 4. For typical combustor exit conditions the error is larger and in some cases unacceptable.

The exact form of Eq. (ii)

$$\frac{p_t'}{p_o} = \frac{1 + 2\frac{q_o}{p_o}\left(1 - \frac{a_o^{*2}}{2u_o^2}\right)}{\left(1 - \frac{\epsilon}{p_t'}\right)} \qquad \text{(iv)}$$

where

$$\frac{\epsilon}{p_t'} = 1 - [4\gamma M_o^2 - 2(\gamma-1)]^{\frac{1}{\gamma-1}} [M_o(\gamma+1)]^{\frac{-2\gamma}{\gamma-1}} \cdot [3\gamma M_o^2 + 2 + \gamma^2 M_o^2] \qquad \text{(v)}$$

can be derived by using the Rankine - Hugoniot relations.

An approximation to Eq. (v)

$$\frac{\epsilon}{p_t'} \approx .012 \left[\frac{2}{(M_o - 0.5)^2} + 1.1 (\gamma - 1.14) \right] \qquad \text{(vi)}$$

adequately describes the ϵ/p_t' correction factor.

Figure A-1 shows the exact and approximate values of ϵ/p_t' as a function of upstream Mach number and average γ. Since the function is only weakly dependent of γ the upstream value can be used and if need be, a first iteration can be made once all of the properties are defined.

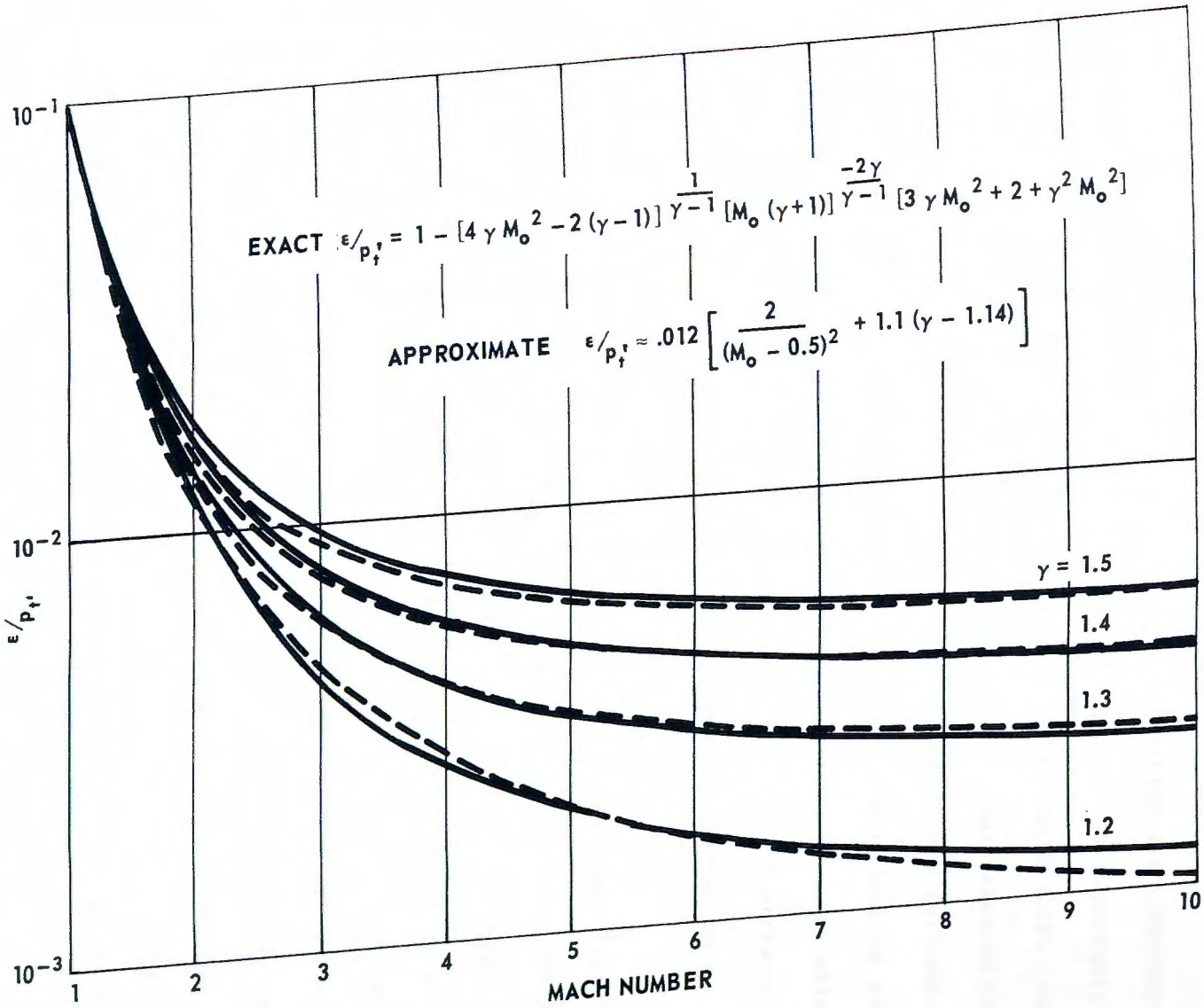

Fig. A-1 Correction Factor for Real Gas Pitot Pressure Ratio

VIII. APPENDIX B

PROPERTIES OF ALUMINUM ALKYL FUELS AND DEFINITION OF COMBUSTION EFFICIENCY

The fuel requirements for supersonic combustion are considerably more stringent than those for subsonic combustion. In supersonic combustion, residence times in the combustion zone are quite short (less than 1 millisecond even in very long configurations), thus reaction rates must be correspondingly more rapid. In subsonic combustors, residence times are considerably greater. Moreover, combustion aids such as bluff body flame stabilizers, spark ignition sources and recirculating piloting devices which are customarily used in subsonic flow are not attractive for use in supersonic flow due to the inherently large disturbances which they create.

The fuel for use in supersonic combustion must therefore be highly reactive and spontaneously ignitible at the prevailing combustor conditions. Additional factors such as cost, availability, thermal stability and handling must also be considered in the selection of the ideal fuel. The aluminum alkyls appear to be a reasonable compromise between cost and reactivity and at the same time have good thermal stability and are not too difficult to handle. These compounds have a wide application in the chemical industry as catalysts for the polymerization of olefins and in the hydrogenation of aromatics. Prices range from $10.00 per lb for trimethyl aluminum (TMA) to $2.00 per lb for triethyl aluminum (TEA) and diethyl aluminum hydride (DEAH). The latter two fuels were used exclusively in these tests.

Some of the more important properties of these fuels are listed in Table III.

TABLE III - PROPERTIES OF TRIETHYL ALUMINUM (TEA) AND DIETHYL ALUMINUM HYDRIDE (DEAH)

PROPERTY	VALUE AND UNITS	
	TEA	66.5% wt TEA 33.5% wt DEAH
Formula	$(C_2H_5)_3Al$	$(C_2H_5)_{2.6}AlH_{0.4}$
Formula Weight	114.2	102.9
Freezing Point	409.8 or 407.5°R (two crystalline forms)	387.3
Boiling Point	827.6°R	842.0
Vapor Pressure @ 600°R	0.015 psia	0.020
@ 672°R	0.250	0.263
@ 744°R	2.124	1.894
Density @ 537°R	6.947 lbs/gal	6.779
@ 761°R	6.148	6.000
Viscosity @ 537°R	2.5 cp	1.9
@ 690°R	7.6	
Specific Heat @ 551°R	.527 Btu/lb°F	.517
Heat of Vaporization @ NBP	216 Btu/lb	193.0
Heat of Combustion, Net @ 537°R	18,352 Btu/lb	18,301
Surface Tension @ 542°R	26.1 Dyne/CM	26.0
@ 690°R	17.7	
Diffusion Coefficient @ 540°R into Air	$\approx$8.6 CM^2/sec	

These properties, with the exception of the diffusion coefficient are from Ethyl Corporation[20] and Koppers Company[21] bulletins. The diffusion coefficient of TEA into air, which was used in the droplet trajectory calculations, was estimated by the technique of Hirschfelder, Curtiss and Bird[22] using estimates of intermolecular spacing from Hirschfelder, et al[22] and Noller[23].

In the performance calculations all species were considered to be in chemical equilibrium at the local flow conditions. The local equilibrium composition was determined by the technique of Browne and Williams[12] on a high speed IBM 7094 computer.

The gas properties at various positions in the 10^{o}-20^{o} ducted combustor for a typical test are listed in Table IV. The location of these positions are shown in Fig. B-1.

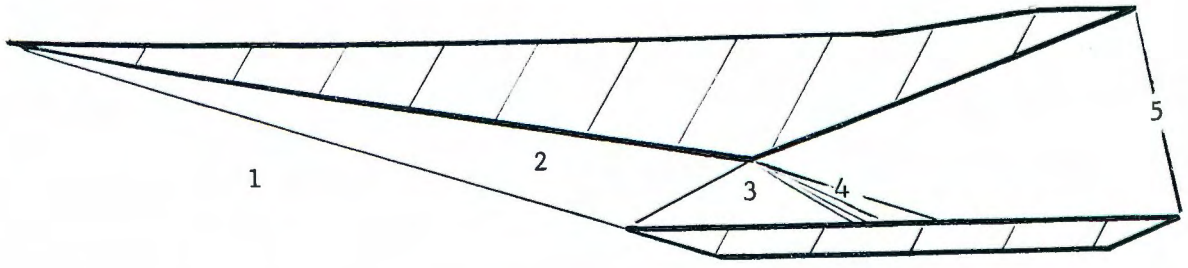

Fig. B-1. Location of Positions for Theoretical Analysis of 10^{o}-20^{o} Ducted Combustor

TABLE IV - GAS PROPERTIES IN TYPICAL TEST OF 10^{o}-20^{o} DUCTED COMBUSTOR

POSITION	LOCATION	STAGNATION TEMPERATURE ^{o}R	STAGNATION PRESSURE PSIA	MACH NO.	STATIC TEMPERATURE ^{o}R	STATIC PRESSURE PSIA
1	Free Stream	2063	110.0	4.90	463	0.22
2	Behind Wedge Oblique Shock	2063	96.3	3.93	533	0.65
3	Behind Cowl Reflected Shock	2063	87.2	3.23	704	1.61
4	Combustor Inlet Plane	2006	87.2	3.85	536	0.61
5	Combustor Exit Plane	2658	21.8	2.95	1057	0.61

The flow from the free stream (1) to the combustor inlet plane (4) is simple two-dimensional wedge flow. Fuel is added in regions (2) and/or (3) but does not begin to release heat until plane (4) is reached. The constant static pressure is maintained from plane (4) to plane (5) by supersonic heat release. The method of determining the amount of fuel required to maintain constant pressure in an increasing area is described in Section III. The gas composition in the combustor exit plane (5) for this theoretically determined case with an equivalence ratio of 0.12 is listed in Table V. Complete combustion is assumed with chemical equilibrium at local conditions.

TABLE V - THEORETICAL CHEMICAL COMPOSITION OF COMBUSTOR EXIT GAS IN TYPICAL TEST OF 10°-20° DUCTED COMBUSTOR

CHEMICAL SPECIES	% BY WEIGHT	CHEMICAL SPECIES	% BY WEIGHT
N_2	74.815	H	10^{-18}
O_2	20.156	$A\ell H_2O$	10^{-24}
CO_2	2.218		
A	1.270		
H_2O	1.114		
$A\ell_2O_3$	.420		
NO	1.8×10^{-4}		
OH	10^{-8}		
O	10^{-12}		
H_2	10^{-14}		
CO	10^{-14}		

Combustion efficiency is defined as the ratio of the theoretical fuel rate required to maintain a given pressure level divided by the actual fuel rate injected in the test.

$$\text{Combustion Efficiency} = \frac{\dot{w}_{f\ \text{THEORETICAL}}}{\dot{w}_{f\ \text{ACTUAL}}} = \frac{ER_{\ \text{THEORETICAL}}}{ER_{\ \text{ACTUAL}}} \qquad \text{(vii)}$$

For the example, given the theoretical ER is 0.12, the actual ER was .655 giving a combustion efficiency of 18.3%. To calculate the various properties at the combustor exit, it is assumed that the gas composition is the same as the theoretically calculated case with an addition of excess unreacted fuel. On this basis, the calculated pitot pressure in the combustor exit plane is 6.98 psia and the measured pitot pressure was 7.03 psia.